LIQUID FLOW STRUCTURE AND MASS TRANSFER IN HORIZONTAL AXIS ROTATING DISKS CONTACTORS I. EXPERIMENTAL AND LIQUID FLOW STRUCTURE RESULTS

Alexandru Dan VASILIU[1], Tanase DOBRE[1,2,*], Cristian Eugen RADUCANU[1], Ciprian Marius ILIE[1]

For countercurrent phases flow in a rotating disks contactor (RDC), in this two-parts work, a cellular model and a combined model plug flow-perfect mixed/plug flow were used to describe the liquid flow structure, while criterial relationships for the characterization of mass transfer kinetics in RDC was selected from several possibilities. Pure carbon dioxide absorption in water was chosen for obtaining values of mass transfer coefficient in liquid phase, corresponding to rotation speed of disks, liquid flow rate and the immersion depth of disks in the liquid. Air humidification was selected for determination of mass transfer coefficients referring to gaseous phase.

Keywords: mass transfer, rotating disks contactors, criterial relationships, partly mass transfer coefficient, experimental methods.

1. Introduction

In order to minimize the mass transfer resistance an effective method for gas-liquid contacting is to generate thin films of liquid that is exposed to gas flow. One of the liquid film generation techniques includes the procedure of forming liquid film on the surface of disks, partially immersed in liquid. The generation of the thin film of liquid takes place by rotating the contactor disks. The disks are partially immersed in the liquid, their upper part being in contact with the gas, which contain one or more components to be transferred to liquid. During the rotational movement, the liquid film formed on the surface of the discs is brought into contact with the gas phase. The width of the liquid film, and therefore the mass transfer surface, depends on the immersion depth of the disks. The main advantage of this design is that the gas-liquid interface is of a known constant size In addition, the contact between the phases is generated by maintaining the liquid phase as a thin film which minimizes the mass transfer resistance, compared to others gas-liquid contacting procedures [1-3]. Areas of use of the rotating disks contactor (RDC) are found especially in bioengineering applications, where the RDC is used as a

[1] Department of Chemical and Biochemical Engineering, Faculty of Chemical Engineering and Biotechnologies, University POLITEHNICA of Bucharest, Romania; tghdobre@gmail.com.
[2] Technical Sciences Academy of Romania

bioreactor for biological wastewater treatment, or for other aerobic bioengineering processes [4, 5] (citric acid by aerobic fermentation, specialized bacterial or fungal cultures, cell cultures, bio cellulose production etc.). The use of RDC in aerobic biochemical processes is based on the fact that a biofilm, containing the system of microorganisms that transforms the substrate (carbon source in the most cases), is formed on the disks surface; that is covered by a mobile film of liquid through which oxygen is transferred to biofilm [6-7]. For the case of biofilm wastewater treatment Fig. 1 shows an enumeration of transfer and bioreaction processes when part of disc contactor surface is rotating in the air (moving from A to B) or rotating in the wastewater being processed (moving from B to C).

The work has two parts. The first part presents the experimental evolution for both parts and the results on liquid-phase flow structure in the RDC. The second part is dedicated to presenting the results obtained in terms of the mass transfer kinetics for the liquid phase and the gas phase when they come into contact in the RDC. Therefore, the two parts have common elements and have the same list of references.

It is obvious that in the complexity of the processes mentioned by exemplification in Fig. 1, can intuit the importance of phases flow structure and of oxygen transfer in gaseous and liquid phase. The current paper focuses on these three aspects. It thus starts from the fact that there is too little information on these aspects, which be taken up in technological design or in simulation, in a concrete case, of an RDC device.

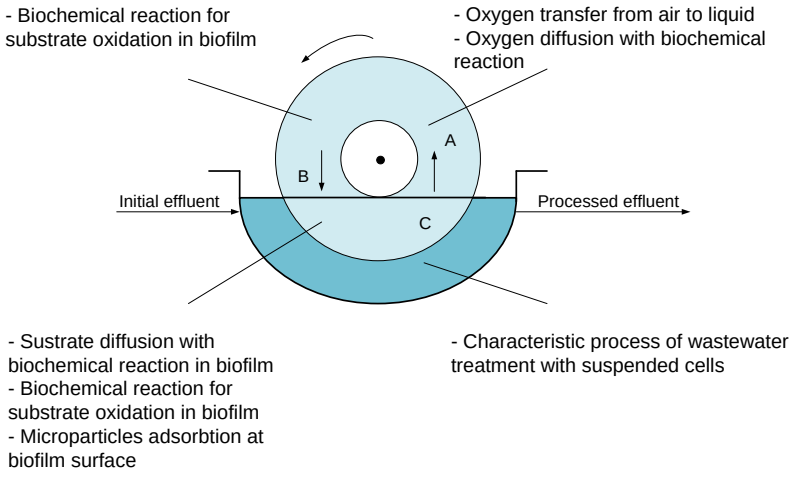

Fig. 1. Processes characterizing the aerobic wastewater treatment in RDC

We thus show that respect to phases flow structure in the RDC, no characteristic data can be found [8], even if from experimental measurements of mass transfer, in closed RDC, it can be deduced that the plug flow (PF) is accepted

for both phases [8, 9]. For RDC open in the atmosphere for oxygenation (Fig. 1) it can formally consider that the gaseous phase has a perfect mixing (PM) flow. For liquid phase the plug flow (PF) could result through a series of PM cells, which are formed between disks, coupled with a PF flow at entry and exit of liquid in/from the RDC [10]. In this paper we accepted the considerations regarding the PF gas flow structure. In respect to liquid phase flow structure, we bring a concrete experimental investigation based on residence time distribution (RTD) measurements when an impulse tracer is applied at liquid input in RDC [10].

In the case of liquid phase mass transfer, the published data follow three directions: i) the application of the renewal theory to this case [7, 11-14], ii) the use of k_l determination method for falling film flow to this case [15], iii) the experimental investigation of process factors influences of on k_l [16, 17], for example by programming experiences. The first direction shows an important influence of the disks rotation speed and of liquid flow rate on liquid phase mass transfer coefficient, k_l, [13, 14]. The second direction also finds cases where the thickness of the liquid film is not really influenced by the usual speed of the disks and the liquid flow rate [18, 19] so that k_l is placed in an area where it has a constant value. The third direction correlates experimental data, and it is dependent on the method of them obtaining [11]. It is worth noting that most of the experimental data used to support the mentioned three directions is based on measuring the oxygenation of the liquid phase, without considering that the neglecting the oxygen transfer resistance in the gaseous phase is not very correct. In our work we use the carbon dioxide absorption from pure gas in RDC, as procedure for correctly determining the k_l and on it process factor influence. Relevant aspects on the modeling of mass transfer in liquid and gaseous phases in a RDC are presented. Mathematical modeling is a valuable tool in designing and optimizing the processes in chemical engineering, as well as in understanding their mechanisms [20-22].

For characterization of the mass transfer kinetics respect to gas phase, practically no data can be found in the literature. In this work the kinetics of air humidification was investigated, for the characterization of mass transfer in the gas phase in RDC phases contacting.

2. Experimental equipment, experimental procedures and methods

The experimental pilot RDC, made of transparent plexiglass, with a diameter of 20 cm, is equipped with 10 plexiglass disks with a diameter of 19 cm and 0.6 cm width. It has nozzles for conveying water and gas (air or carbon dioxide) and the disks shaft is sealed with fine packing. An electric motor, powered by a voltage-controlled system, ensures the rotation of the disks with controlled speed, established by means of a belts speed reducer.

Fig. 2 shows how the RDC was equipped to enable the three mentioned experimental investigations: i) to identify the liquid phase flow structure through the RDC; ii) to characterize the influence of process factors on the kinetics of liquid phase mass transfer in RDC; iii) establishing the influence of process factors on the mass transfer kinetics in the gas phase.

2.1. Experimental Residence Time Distribution

It is known that Danckwerts [23] approached the study of fluid flow in reactors and others equipment in a brilliant and simple way: *introduce a pulse of tracer into the fluid entering the reactor (equipment) and see when it leaves*. The normalized outlet tracer concentration versus time, $E(\tau)$, is the Residence Time Distribution (RTD). Here the normalized outlet concentration is the momentary tracer outlet concentration, $c_{tr\ out}(\tau)$ normalized by the area under the curve $c_{tr\ out}(\tau)$ versus time (τ).

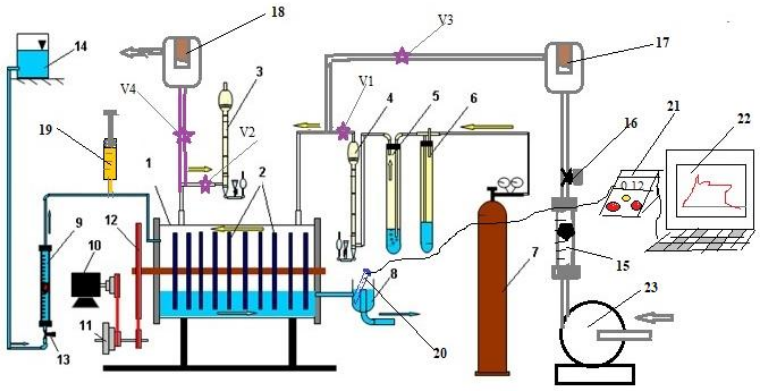

Fig. 2. Experimental device for investigation of liquid flow structure, mass transfer in liquid phase and mass transfer in gas phase at countercurrent phases contacting in a RDC:

1. Rotating disks contactor with 10 disks; 2. Disks in contactor; 3. Soap bubble flow meter for carbon dioxide exit; 4. Soap bubble flow meter for carbon dioxide input; 5. Bubbler for carbon dioxide saturation with water; 6. Manostat; 7. Carbon dioxide bottle; 8. Hydraulic water shut-off; 9. Rotameter for water flow rate; 10. Electric motor; 11. Speed reducer; 12. Disk system drive wheel; 13. Valve for absorbent (water) liquid flow rate; 14. Constant level water reservoir; 15. Rotameter for air; 16. Valve for air flow control; 17. Data logger for air humidity at the RDC input; 18. Data logger for air humidity at the RDC exit; 19. Tracer injection syringe (NaCl solution 36 g/L); 20. Conductometric probe; 21. *Fischer Scientific* conductometer with RS 232 interface; 22. Data storage/processing computer; 23. Air fan; V1, V2, V3 ,V4 – valves for selecting of experimental procedure.

The relation (1) express E(τ). For discrete points measurement E(τ) becomes by means of relation (2), where it observes that the integral from relation (1) in

numerically computed considering N measured data for $c_{tr\ out}$ or time, strung with step $\Delta\tau$.

$$E(\tau) = \frac{c_{tr\,out}(\tau)}{\int_0^{\infty} c_{tr\,out}(\tau)} \tag{1}$$

$$E(\tau_i) = \frac{c_{tr\,out}(\tau_i)}{\left[c_{tr\,out}(\tau_0) + 2\sum_{i=0}^{i=N-1} c_{tr\,out}(\tau_i) + c_{tr\,out}(\tau_N)\right]\frac{\Delta\tau}{2}} \tag{2}$$

In respect to Fig. 2, the experimental arrangement for $E(\tau)$ building does not use CO_2 line. For an experiment, the liquid volume (V_l) in RDC, the liquid flow rate (G_{vl}) and the disks rotation speed (n) are fixed. As tracer 36 g/L NaCl solution was used, it obtains impulse input of tracer in RTD by instant injection of a 10 mL NaCl solution volume (syringe 19 in Fig. 2) into water input in RDC. The on-line registration of tracer dynamics at the RDC exit, by mean of chain conductometric probe (20)/conductometer (21)/computer (22), offers the curve $c_{trout}(\tau_i)$. The evolution curves for tracer concentration at the contactor exit, obtained for different combination of operating parameters values (liquid flow rate, RDC liquid dowry and disc rotation speed), were processed on basis of selected combined models. Table 1 shows the values of the process factors considered in obtaining the experimental curves $c_{tr\ out}(\tau_i)$.

Table 1

Process factors for NaCl tracer dynamics at the RTD exit for it impulse input

Process Factors	Values of specific units			
Rotation speed [rot/min]	4	14	24	34
Liquid volume in RTD, [L]	1.25	2.9	5.2	6.0
Liquid flow rate in RTD, [L/min]	24	30	36	52
Air flow rate in RTD, [L/min]	500			
Experimental conditions	t= 25^{0}C, p= 760 mmHg			

$$n_A = k_l A \Delta c_{Am,} \tag{3}$$

$$\Delta c_{Am} = \frac{\left(c_A^* - c_{A\,out}\right) - \left(c_A^* - c_{A\,inp}\right)}{\ln\left(\frac{\left(c_A^* - c_{A\,out}\right)}{\left(c_A^* - c_{A\,inp}\right)}\right)} = \frac{c_{A\,oiut}}{\ln\left(\frac{c_A^*}{c_A^* - c_{A\,out}}\right)} \tag{4}$$

$$c_{A\,out} = \frac{n_A}{G_{vl}} \tag{5}$$

$$A = \left(\frac{\pi D + \pi (D - h)}{2} \right) \cdot h \cdot \left(\frac{360 - \theta(h)}{360} \right) \tag{6}$$

$$\theta(h) = 2 \arccos\left(\frac{D - 2h}{D} \right) \tag{7}$$

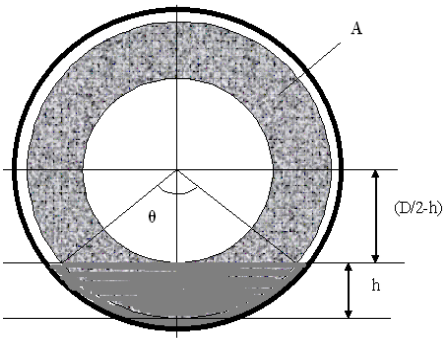

Fig. 3. The geometry of mass transfer area development

Carbon dioxide is hardly soluble, so great care is needed to measure the absorbed carbon dioxide flow rate [24]. It was thus chosen to measure the carbon dioxide entering flow rate in RDC and the one leaving it. It used soap bubble flowmeters (3, 4 in Fig. 2), because these flow rates have very low values. The experimental investigation was organized according to an experimental plan with factors at two levels.

Table 2

Process Factors Levels at investigation of liquid phase mass transfer kinetics

Exp./ Name	Natural process factors			Dimensionless process factors		
	Liquid velocity $w_l \cdot 10^4$ [m/s]	Disks rotation speed n [sec^{-1}]	Disks immersion depth h [m]	X_1	X_2	X_3
1	4.42	0.4	0.045	+1	-1	-1
2	4.42	0.4	0.090	+1	-1	+1
3	4.42	0.8	0.045	+1	+1	-1
4	4.42	0.8	0.090	+1	+1	+1
5	8.84	0.4	0.045	-1	-1	-1
6	8.84	0.4	0.090	-1	-1	+1
7	8.84	0.8	0.045	-1	+1	-1
8	8.84	0.8	0.090	-1	+1	+1
9	6.63	0.6	0.062	0	0	0
10	6.63	0.6	0.062	0	0	0
11	6.63	0.6	0.062	0	0	0
Experimental conditions: t = 25^0C, p = 760 mmHg						

It takes into account that the liquid flow rate, expressed by correspondent *fictive liquid velocity*, *the rotation speed of discs* and t*he liquid immersion depth of the discs*, are the factors with the greatest influence in k_l determining. Table 2 gives the natural and dimensionless levels of the factors considered in our experimental investigation.

2.2. Mass Transfer Kinetics for Gaseous Phase

The experimental investigation developed for mass transfer investigation for gaseous phase was based on *air humidification*. In this case the mass transfer resistance is only in gas phase because at liquid surface there is a saturation pressure of the water vapors, leading thus to the equality between the total mass transfer coefficient, K_g and partly gas phase mass transfer coefficient, k_g. In an experiment, as shown in Fig. 2, the measurement of the air flow rate and its humidity at input (data logger 17) and exit (data logger 18) in/from the RDC allows obtaining the flow rate of water vapor transferred from liquid (water) to gas (air).

Table 3

Air characteristics for input and exit in/from RDC at beginning of an experiment

	Air input in RDC			Air exit from RDC		
Time [min]	t_g [^{0}C]	RH [%]	t_{dp} [^{0}C]	t_g [^{0}C]	RH [%]	t_{dp} [^{0}C]
1	27.4	24.2	5.1	27.1	61.2	19.0
2	27.2	23.3	4.4	26.8	61.5	18.8
3	27.0	23.7	4.5	26.4	62.3	18.6
4	26.7	24.5	4.7	26.0	62.5	18.3
5	26.5	26.3	5.6	25.8	63.3	18.3
6	26.3	24.9	4.6	25.5	63.3	18.0
7	26.2	24.7	4.4	25.4	63.6	18.0
8	26.0	26.8	5.4	25.3	64.3	18.1
9	25.9	27.9	5.9	25.1	64.5	17.9
10	25.9	26.3	5.1	25.0	65.1	18.0
11	25.8	26.8	5.2	24.8	65.2	17.8
12	25.8	26.5	5.1	24.7	65.2	17.8
Experimental conditions: p =760 mmHg, Air flow rate G_{vg} = 1500 L/h, Water flow rate G_{vl} = 80 L/h, Rotation speed of disks n = 24 min^{-1}, Immersion depth of disks h = 0.045 m, Monitored water temperature: t_w = 24 ^{0}C,						

In this transfer case the local driving force is expressed by relation (8), where equilibrium molar fraction and local molar faction of water vapors are given by relations (9) and (10). In (9) and (10) the temperature liquid (water) (t_w) is the mean of measured at input and exit of liquid in/from RDC and the air relative humidity are provided (measured) by the data logger.

$$\Delta y = y^*(t_w) - y \tag{8}$$

$$y^*(t_{dp}) = \frac{p_{sv}(t_w)}{p} \tag{9}$$

$$y = \frac{U_r}{100} y^*(t_w) \tag{10}$$

Table 3 shows a sequence of data provided by data loggers in one experiment. From the data showed in Table 3 the four important process factors of mass transfer kinetics were identified. They are: i) air flow rate, G_{vg}, or in intensive form gas fictive velocity, w_g; ii) liquid (water) flow rate, G_{vl}, or in intensive form liquid fictive velocity, w_l; iii) rotation speed of disks, n; iv) immersion depth of disks, h.

The set of following (11)–(17) relations (where mass transfer area is established as it is shown by relations (6) and (7), where the saturation pressure of water vapors from $y^*(t_w)$ is given, in Pa, by relation (18) [25]), describes the data processing in order to obtain partly mass transfer coefficient for gas phase.

$$y_{in} = \frac{RH_{in}}{100} y^*(t_w) \tag{11}$$

$$y_{out} = \frac{RH_{out}}{100} y^*(t_w) \tag{12}$$

$$n_A = \frac{G_{vg}}{22.4} \frac{273}{273 + t_g} (y_{out} - y_{\text{int}}) \tag{13}$$

$$\Delta y_{in} = \frac{y_{out} - y_{in}}{\ln\left(\frac{y^*(t_w) - y_{\text{int}}}{y^*(t_w) - y_{out}} \right)} \tag{14}$$

$$k_y = \frac{n_A}{\Delta y_{in}} \tag{15}$$

$$C = \frac{p}{R(t_g + 273)} \tag{16}$$

$$k_{cg} = \frac{k_y}{C} \tag{17}$$

$$p_{sv}(t) = 707.303 - 27.036t + 4.3608t^2 - 0.0466t^3 + 0.00103t^4 \tag{18}$$

With reference to Fig. 2, the execution of an experiment follows these steps: i) ensure the closure of the carbon dioxide supply line in the installation; ii) set the air flow rate at value characteristic for the experiment; iii) set the liquid flow rate

(water) at selected level; iii) by maneuvering the hydraulic closure (8 in Fig. 2) in the vertical plane, the depth of discs immersion in liquid is established; iv) the rotation speed of the discs is fixed at desired value; v) the data loggers are set, started and placed in their locations (17 and 18 in Fig. 2); vi) the inlet and outlet temperatures of the water from the RDC are measured during of experiment; vii) the installation is maintained in the chosen state about 20 minutes to be sure that the steady state transfer is obtained.

Table 4

Process Factors Levels at investigation of gas phase mass transfer kinetics

Exp./ Name	G_{vl} [L/h]	$w_l \cdot 10^4$ [m/s]	G_{vg} [L/h]	$w_g \cdot 10^2$ [m/s]	n [min^{-1}]	h [cm]	X_1	X_2	X3	X_4
1	80	7.07	1200	1.10	0.4	9.00	+1	+1	-1	+1
2	80	7.07	1200	1.10	0.4	4.50	+1	+1	-1	-1
3	80	7.07	1200	1.10	0.8	9.00	+1	+1	+1	+1
4	80	7.07	1200	1.10	0.8	4.50	+1	+1	+1	-1
5	80	7.07	600	0.55	0.4	9.00	+1	-1	-1	+1
6	80	7.07	600	0.55	0.4	4.50	+1	-1	-1	-1
7	80	7.07	600	0.55	0.8	9.00	+1	-1	+1	+1
8	80	7.07	600	0.55	0.8	4.50	+1	-1	+1	-1
9	40	3.54	1200	1.10	0.4	9.00	-1	+1	-1	+1
10	40	3.54	1200	1.10	0.4	4.50	-1	+1	-1	-1
11	40	3.54	1200	1.10	0.8	9.00	-1	+1	+1	+1
12	40	3.54	1200	1.10	0.8	4.50	-1	+1	+1	-1
13	40	3.54	600	0.55	0.4	9.00	-1	-1	-1	+1
14	40	3.54	600	0.55	0.4	4.50	-1	-1	-1	-1
15	40	3.54	600	0.55	0.8	9.00	-1	-1	+1	+1
16	40	3.54	600	0.55	0.8	4.50	-1	-1	+1	-1
17	60	4.72	900	0.71	0.6	6.75	0	0	0	0
18	60	4.72	900	0.71	0.6	6.75	0	0	0	0
19	60	4.72	900	0.71	0.6	6.75	0	0	0	0
20	60	4.72	900	0.71	0.6	6.75	0	0	0	0

As it follows from the above, 4 factors influenced the mass transfer kinetics in the gas phase. It was thus decided to organize the experimental investigation with a factorial plan with two levels for each factor. Table 4 shows the natural state of process factors as well as their dimensionless expression. For air and water (liquid) flow rate, it gives the extensive (flow rate in normal units), and intensive (fictive velocities) values. Also, it observes from Table 4 that, we have for experiments in the center of factorial plan and that is used in order to establish the reproducibility variance of experimental procedure.

3. Results and discussions

Fig. 4 and 5 show the measured response of NaCl concentration dynamics at the exit from the RDC, when a unit pulse of tracer (NaCl), with its concentration of 36 g/L, was applied at RDC liquid (water) input. We thus observe that three process factors (fictive liquid velocity, rotation speed of the disks and immersion depth of disks in liquid) influenced the concentration dynamics at the exit from the RDC, as well as the presence of an important mixting, highlighted by these curves.

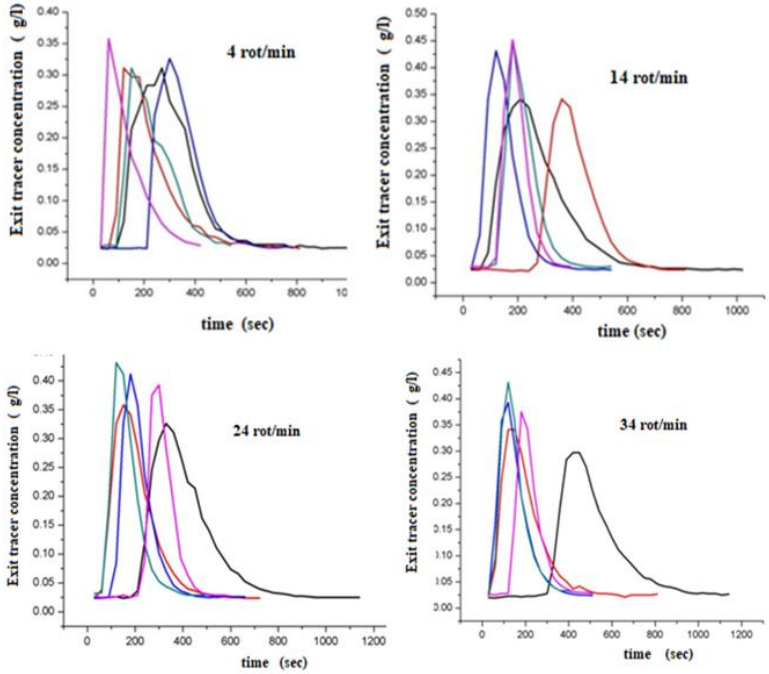

Fig. 4. Influence of disks rotation speed and liquid flow velocity on RDC tracer exit dynamics for disks immersion depth of 0.03 m (black - w_l = 0.00022 m/s, red - w_l = 0.000265 m/s, blue - w_l = 0.000313 m/s, green - wl = 0.000375 m/s, turquoise - w_l = 0.000433 m/s)

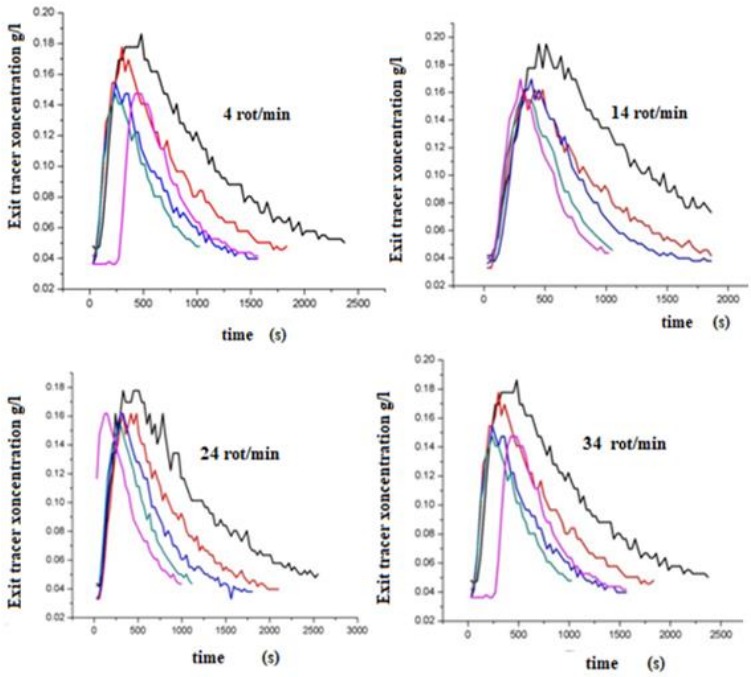

Fig. 5. Influence of disks rotation speed and liquid flow velocity on RDC tracer exit dynamics for disks immersion depth of 0.09 m (black - w_l = 0.00022 m/s, red - w_l = 0.000265 m/s, blue - w_l = 0.000313 m/s, green - w_l = 0.000375 m/s, turquoise - w_l = 0.000433 m/s)

At the same time, the beginning part of the curves and their end part show the presence of a plug flow liquid displacement in the RDC global flow. At a first analysis of tracer concentration curves at the exit from the DRC, it is found: i) all process factors participate in development of these curves; ii) by the fact that all the curves show a displacement in time of their beginning and then a kind of plateau at their end, it is appreciated that this fact indicates that in these positions a plug flow model is present; iii) the main part of these curves clearly indicates a strong participation in their formation of the flow with perfect entanglement; iv) the existence of small stagnant areas in the DRC is not excluded.

Now, if it accepts that the perfect mixing is strong in the curves giving tracer exit dynamics from RDC, then it can be applied to a cellular model with perfectly mixed identical cells, which can well describe the liquid phase flow structure in RDC (Fig. 5).

However, as shown by the mathematical model of this flow structure [26], given by relations (19) - (22), it cannot predict the influence of disks rotation speed on the exit curves of the tracer from the RDC.

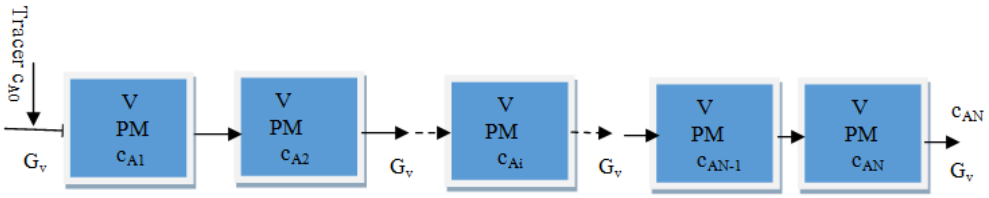

Fig. 6. Cellular model for liquid flow structure in RDC

$$\frac{dc_{A1}}{d\tau} = -\frac{G_v}{V}\left(c_{A1} - c_{A0}\right) \tag{19}$$

$$\frac{dc_{Ai}}{d\tau} = -\frac{G_v}{V}\left(c_{Ai} - c_{Ai-1}\right) \text{i} = 1,2....\text{N} \tag{20}$$

$$\frac{dc_{AN}}{d\tau} = -\frac{G_v}{V}\left(c_{AN} - c_{AN-1}\right) \tag{21}$$

$$c_{A0} = \frac{c_{A0} \text{ for } 0 \le \tau_{\text{in}}}{0 \text{ for } \tau \succ \tau_{\text{in}}} \tag{22}$$

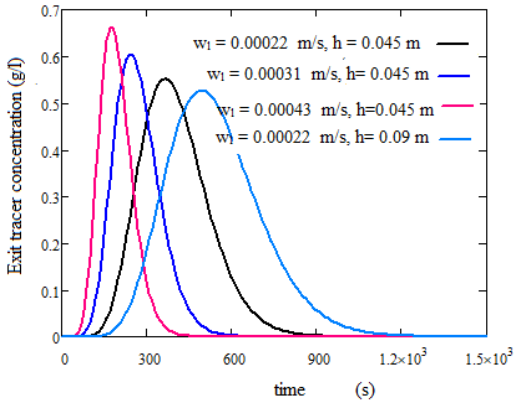

Fig. 7. The exit tracer concentration from RDC simulated by cellular model

Fig. 7, based on the cellular model, even if it correctly shows the influence of the liquid velocity (liquid flow rate) and the immersion depth of disks in liquid (the volume of liquid from contactor), cannot, as announced, explain the influence of disks rotation speed on the flow structure of the liquid phase through RDC. We thus establish that a combined model (CM) is needed. In CM the size of the parts is also dependent on the intensity of the disks' rotation. Thus, the model from Fig. 8

is considered, where the plug flow and perfect mixed flow are in series and where the perfect mixed flow is coupled with a small stagnant (dead) zone.

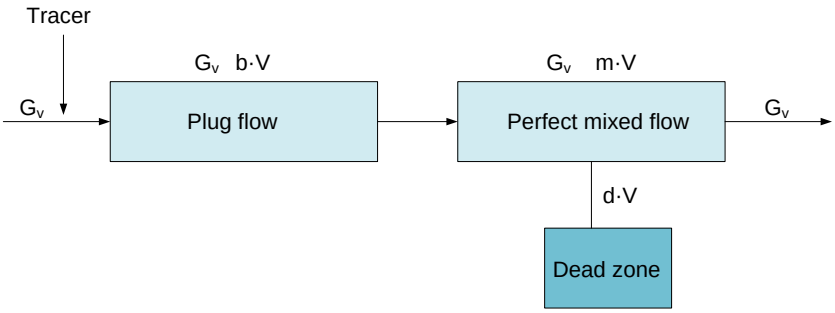

Fig. 8. Combined model for liquid flow structure in RDC

$$C(\theta) = \frac{c_{out}(\theta)}{c_0} = 1 - \exp\left(-\frac{1}{m}(\theta - b)\sigma(\theta - b) \right) \tag{23}$$

$$\sigma(\theta - b) = \frac{0 \; for \; \theta \le \mathrm{b}}{1 \; \mathrm{for} \; \theta \succ \mathrm{b}} \tag{24}$$

$$\ln\left(1 - C(\theta_i)\right) = -\frac{1}{m}\theta_i\sigma(\theta_i - b) + \frac{b}{m}\sigma(\theta_i - b) \tag{25}$$

$$m + b + d = 1 \tag{26}$$

Fig. 9, which shows how the process factors influence the three participations in the formation of the liquid phase flow structure in the RDC shows that: i) predominantly (over 85% and increasing with disks rotation speed, with liquid flow rate and with volume of liquid in the contactor (disks immersion depth)) in RDC the flow of liquid is of perfect mixing type; ii) the participation of plug flow in structure does not exceed 10% and is decreasing, up to 2%, with all 3 process factors; iii) the presence of the dead zone in the flow structure is modest

If some of the data in Fig. 8 will be considered in an experimental arrangement with 3 factors at two levels with *m* and *b* as answers, then it is possible to express it by relationships that show their dependence on process factors.

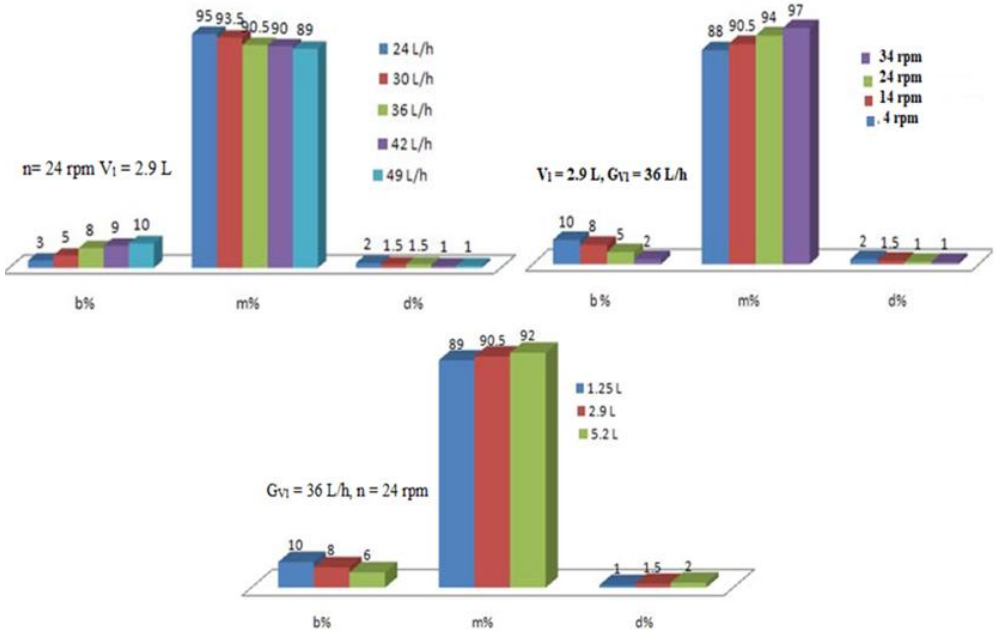

Fig. 9. Influence of process factors on liquid flow structure in RDC described by the combined model from Fig. 7

Table 5 contains these data. With these data, *b* and *m* are expressed through a regression function after X_1, X_2 and X_3 that contains a free term, linear dependence terms, binary and ternary interaction terms [27].

Table 5

Matrix of experimental plan 2^3 for *m* and *b* dependency upon of X_1, X_2 and X_3

Exp./ Name	Natural process factors			Dimensionless factors			*m* [%]	*b* [%]
	$w_l \cdot 10^4$ [m/s]	*n* [sec^{-1}]	h/D	X_1	X_2	X_3		
1	1.372 (24 L/h)	0.058 (4 rpm)	0.250	+1	-1	-1	86	11
2	1.372 (24 L/h)	0.058 (4 rpm)	0.500	+1	-1	+1	87	10
3	1.372 (24 L/h)	0.400 (24 rpm)	0.250	+1	+1	-1	90	8
4	1.372 (24 L/h)	0.400 (24 rpm)	0.500	+1	+1	+1	95	4
5	3.251 (48 L/h)	0.058 (4 rpm)	0.250	-1	-1	-1	85	12
6	3.251 (48 L/h)	0.058 (4 rpm)	0.500	-1	-1	+1	89	8
7	3.251 (48 L/h)	0.400 (24 rpm)	0.250	-1	+1	-1	91	7
8	3.251 (48 L/h)	0.400 (24 rpm)	0.500	-1	+1	+1	92	7
9	2.456 (36 L/h)	0.233 (14 rpm)	0.375	0	0	0	90	8
10	2.456 (36 L/h)	0.233 (14 rpm)	0.375	0	0	0	91	7
11	2.456 (36 L/h)	0.233 (14 rpm)	0.375	0	0	0	90	9

It is worth noting that in table 6 there are three replicated measurements in the center of the experimental plan. Their purpose is to calculate the experimental reproducibility variance, who is used to eliminate from the general statistical model (8 terms in the present case) all terms that are not significant for a confidence level $1-\alpha = 0.95$. The analysis of data from table 6 with a specific software, based on this specific procedure for the organization of this type of experimental investigation [18], leads for *m* and *b* to expressions (28) respectively (29).

$$m = 89.375 + 0.315\,X_1 + 2.625\,X_2 + 1.375\,X_3 \tag{27}$$

$$b = 8.375 - 1.875\,X_2 - 1.125\,X_3 \tag{28}$$

$$X_1 = \frac{w_l - 0.0002556}{0.0000819} = \frac{G_{vl} - 36}{12}, \mathrm{X}_2 = \frac{n - 0.233}{0.167}, X_3 = \frac{h/D - 0.375}{0.125} \tag{29}$$

We note that the relationships obtained show only individual influence of process factors (w_l, *n*, *h*) on the components (*b*, *m*) of the combined model that was considered in the valorization of the experimental data. Since in X_1, X_2 and X_3, factors with intensive expression were used, relations (27) and (28) can be used for any up-scaling of the liquid phase flow structure in the RDC. It is worth noting that even at low speeds of the disks, the proportion of perfect mixing in the flow structure of liquid phase through the RDC is over 80%. This agrees with many data from the literature when it is accepted for wastewater treatment in disks contactors plants that the liquid phase is perfectly mixed [5-7, 28, 29]

4. Conclusions

Although the use of RDC is presented in many physical, chemical, and biochemical applications (air conditioning, gas-liquid reactions, blood oxygenation, tissue culture, and biological wastewater treatment) there is a lack of a systematic approach to characterize the flow and mass transfer in such equipment. Using experimental investigation and mathematical modeling, the current work pursued the characterization of liquid phase flow as well as the expression of the mass transfer kinetics in liquid and gaseous phases in RDC contacting. Respect to the first problem, it is shown that:

- a pilot laboratory device was created and equipped in such a way as to allow the following:

  a) investigating of liquid phase flow structure by mean of tracer pulse method;

  b) characterization of the mass transfer kinetics in liquid phase through absorption of pure CO_2 by water;

c) identification of the mass transfer kinetics for gaseous phase through air humidification.

- the liquid flow structure measurements showed that the liquid velocity, the disks rotation speed and the depth of their immersion in the liquid are process factors, such that: a) the valorization of the measurements through a perfectly mixed model with equal cells does not highlight the role of disks rotation speed in structure of liquids phase flow; b) the combined flow model, with total displacement in series with perfect mixing with dead space, allowed the measurements to be well utilized; c) the factorial organization of the experimental investigation allowed the expression of the combined model parameters as functions of the process factors.

Aknowledgement

This work has been funded by the European Social Fund from the Sectoral Operational Programme Human Capital 2014-2020, through the Financial Agreement with the title "Training of PhD students and postdoctoral researchers in order to acquire applied research skills - SMART", Contract no. 13530/16.06.2022 - SMIS code: 153734.

R E F E R E N C E S

[1]. *A. J. Zeevalkink, P. Kelderman, C. D. Visser, C. Boelhouwer,* Physical Mass Transfer in Rotating Disc Gas-Liquid Contactor, Water Research, **vol. 13**, (5), 1979, pp. 913-919.

[2]. *D. Hualing, Z. Kun, L. Houfang, L. Changjun, W. Keijing, L. Yingying, CO_2* Absorption in an Rotating Disk Reactor Using DBU-Glycerol as Solvent, Chinese Journal of Chemical Engineering, **vol. 28**, 2020, pp. 104-113.

[3]. *P. K. Hsueh, J. O. Hao, C. Y. Wu,* Removal of Volatile Organic Compounds in a Rotating Disk Contactor: Batch and Continuous Operation, Journal of Water Pollution Control Federation, **vol. 63**, (1), 1991, pp. 67-74.

[4]. *Dutta Sanjay,* Mathematical Modeling of the Performance of a Rotating Biological Contactor for Process Optimisation in Wastewater Treatment, PhD Thesis, Karlsruhe University, ISBN 978-3-9809383-9-6, 2007.

[5]. *A. A. Friedman,* Effect of Disk Rotational Speed on Biological Efficiency, Journal of Water Pollution Control Federation, **vol. 51**, 1979, pp. 2678 – 2690.

[6]. *S. J. Melo, S. Kholi, W. A. Patwardhan, S. D. F. Souza,* Effect of oxygen transfer limitations in phenol biodegradation, Process Biochemistry Elsevier, **vol. 40**, 2004, pp. 625-628.

[7]. *T. Yamane, F. Yoshida,* Absorption in a Rotating Disk Gas-Liquid Contactor, Journal of Chemical Engineering of Japan, **vol. 5**, (4), 1972, pp. 381- 385.

[8]. *P. R. Kalnache, R. V. D. Murthy, A. Achor, K. Reval,* Residence Time Distribution Studies in a Rotating Packed Disk Contactor: Mathematical Modeling and Validation, International Journal of Chemical Reactor Engineering, 201190101, 2020, pp. 1-12.

[9]. *S. Cortez, P. Teixeira, R. Oliveira, M. Mota*, Rotating Biological Contactors: A Review on Main Factors Affecting Performance, Reviews in Environmental Science and Bio/Technology (Online), **vol. 7**, (2), 2008, pp. 155–172.

[10]. *G. Xiaofeng, F. Yilin, L. Lingai*, Residence time distribution on flow characterisation of multichannel systems: Modelling and experimentation, Experimental Thermal and Fluid Science, **vol. 99**, 2018, pp. 407 – 419.

[11]. *H. M. Bintanja, J. V. M. Vandererve, C. Boelhouwer*, Oxygen transfer in a rotating disc treatment plant, Water Res., **vol. 9**, 1975, pp. 1147–1153.

[12]. *S. K. Gupta, K. S. Vijary*, Model for oxygen Transfer in Rotating biological contactor, Journal of Chemical Technology and Biotechnology, **vol. 87**, (4), 2012, pp. 540- 545.

[13]. *R. N. Vaidya, G. V. Pangarkar*, Hydrodynamics and Mass Transfer in a Rotating Biological Contactor, Chemical Engineering Communication, **vol. 39**, (1-6), 1985, pp. 337-354.

[14]. *J. Chin*, A Theoretical Analysis on the Biofilm Reactors, Inst. Chem. Engrs., **vol. 34**, (6), 2003, pp. 643-653.

[15]. *K. Afanasiev, A. Munch, B. Wagner*, Thin film dynamics on a vertically rotating disk partially immersed in a liquid bath, Science Direct, Applied Mathematical Modelling, **vol. 32**, 2008, pp. 1894-1911.

[16]. *B. E. Boumansour, J. L. Vasel*, A new tracer gas method to measure oxygen transfer and enhancement factor on RBC, Water Res., **vol. 32**, (4), 1998, pp. 1049–1058.

[17]. *V. Kubsad, S. Chaudhari, S. K. Gupt*a, Model for oxygen transfer in rotating biological contactor. Water Research, **vol. 38**, 2004, pp. 4297 – 4304.

[18]. *A. J. Zhevalkink, P. Kelderman, C. Boelhouwer*, Liquid film thickness in a rotating disc gas-liquid contactor, Water Research, **vol. 12**, (8), 1978, pp. 577-581.

[19]. *N. Hendrasarie, T. Nurtona, Hermana J.*, Experimental Study of the Liquid Film Flow on Rotating Disc Contactor of Rough Surface Partially Immersed in Liquid Bath, International Journal of ChemTech Research, **vol. 10**, (6), 2017, pp. 1-9.

[20]. *T. Dobre, O.C. Pârvulescu, A. Stoica-Guzun, M. Stroescu, I. Jipa, A.A.A. Al Janabi*, Heat and mass transfer in fixed bed drying of non-deformable porous particles, Int. J. Heat Mass Transfer, **vol. 103**, 2016, pp. 478-485.

[21]. *T. Dobre, O.C. Pârvulescu, J. Sanchez-Marcano, A. Stoica, M. Stroescu, G. Iavorschi*, Characterization of gas permeation through stretched polyisoprene membranes, Sep. Purif. Technol., **vol. 82**, 2011, pp. 202-209.

[22]. *T. Dobre, L.R. Zicman, O.C. Pârvulescu, E. Neacşu, C. Ciobanu, F.N. Drăgolici,* Species removal from aqueous radioactive waste by deep-bed filtration, Environ. Pollut., **vol. 241**, 2018, pp. 303-310.

[23]. *P.V. Danckwertz*, Continuous Flow Systems: Distribution of Residence Times, Chemical Engineering Science, **vol. 2**, (1), 1953, pp. 1-13.

[24]. *O. Floarea, R. Dima*, Mass Transfer and Specific Equipment, Chapter Interphase Transfer, Didactic and Pedagogical Publishing House, Bucharest, 1984.

[25]. Z. *Wang, Z. Jia, R. Li, Q. Gao, Z. Gu*, Analysis and Experimental Study on Water Vapor Partial Pressure in the Membrane Distillation Process, Membranes, **vol. 12**, (802), 2022, pp.1-18.

[26]. *R. Stokes, L. Nauman, E. Bruce*, Residence Time Distribution Functions for Stirred Tanks in Series, Canadian Journal of Chemical Engineering, **vol. 48**, (6), 1970, pp. 723–725.

[27]. *O. Munteanu, A. Woinaroschi, G. Bozga*, Applications to Computation of Chemical Reactors, Chapter Residence Time Distribution,Technical Publishing House, Bucharest, 1984.

[28]. *T. Dobre, J. M. Sanchez*, Chemical Engineering Modeling Simulation and Similitude, Chapter Statistical Modelling, Wiley VCH, 2007.

[29]. *J. O. Hao, P.A. Davis*, Modelling of Volatile Organic Compounds Stripping in Rotating Disk Contactor System, Environ. Sci. Technol., **vol. 25**, (11), 1991, pp. 1891-1896.